The *in situ* bacterial production of fluorescent organic matter; an investigation at a species level.

Authors

B.G. Fox[1], R.M.S. Thorn[1], A.M. Anesio[2], and D.M. Reynolds[1]

Affiliations

[1]Centre for Research in Biosciences, University of the West of England, Bristol, BS16 1QY, UK

[2]School of Geographical Sciences, University of Bristol, Bristol, BS8 1SS, UK

Abstract

Aquatic dissolved organic matter (DOM) plays an essential role in biogeochemical cycling and transport of organic matter throughout the hydrological continuum. To characterise microbially-derived organic matter (OM) from common environmental microorganisms (*Escherichia coli, Bacillus subtilis* and *Pseudomonas aeruginosa)*, excitation-emission matrix (EEM) fluorescence spectroscopy was employed. This work shows that bacterial organisms can produce fluorescent organic matter (FOM) *in situ* and, furthermore, that the production of FOM differs at a bacterial species level. This production can be attributed to structural biological compounds, specific functional proteins (e.g. pyoverdine production by *P. aeruginosa*), and/or metabolic by-products. Bacterial growth curve data demonstrates that the production of FOM is fundamentally related to microbial metabolism. For example, the majority of Peak T fluorescence (> 75%) is shown to be intracellular in origin, as a result of the building of proteins for growth and metabolism. This underpins the use of Peak T as a measure of microbial activity, as opposed to bacterial enumeration as has been previously

suggested. This study shows that different bacterial species produce a range of FOM that has historically been attributed to high molecular weight allochthonous material or the degradation of terrestrial FOM. We provide definitive evidence that, in fact, it can be produced by microbes within a model system (autochthonous), providing new insights into the possible origin of allochthonous and autochthonous organic material present in aquatic systems.

Highlights

- Peak T fluorescence is a proxy for microbial activity rather than enumeration.
- Peak T is mainly intracellular material but does exist as extracellular FDOM.
- FOM associated with high molecular weight compounds can be autochthonous in origin.
- A range of FOM peaks are derived from both allochthonous and autochthonous sources.
- Extracellular microbial FDOM is a key source of organic matter in aquatic systems.

Keywords

Dissolved organic matter; *In situ* microbial processing; Excitation-Emission Matrix fluorescence spectroscopy; Fluorescent organic matter; Autochthonous; Allochthonous

Abbreviations

OM – organic matter; DOM – dissolved organic matter; EEM – excitation-emission matrix; FOM – fluorescent organic matter; FDOM – fluorescent dissolved organic matter; QSU – quinine sulphate units; PARAFAC – parallel factor analysis; OD – optical density; *E. coli* – *Escherichia coli; B. subtilis – Bacillus subtilis*; *P. aeruginosa – Pseudomonas aeruginosa*

1 Introduction

Dissolved organic matter (DOM) in aquatic systems plays an essential role in global biogeochemical cycling (Bieroza and Heathwaite, 2016; Hudson et al., 2007). It is generally accepted that the majority of DOM found in freshwaters is allochthonous, with a proportion of the DOM considered to be produced *in situ*, i.e. autochthonous material (Coble et al., 2014). Fluorescence excitation-emission matrix (EEM) spectroscopy has been increasingly employed in recent research to characterise aquatic fluorescent organic matter (FOM) and fluorescent dissolved organic matter (FDOM) (Baker, 2005; Bridgeman et al., 2015). The use of this technique has advanced our understanding of FDOM, its classification, transformation and potential origin (Hudson et al., 2007; Stedmon and Bro, 2008).

Aquatic FDOM has been characterised as consisting of humic-like material considered to be of allochthonous origin of terrestrial input (Coble et al., 2014). The compounds associated with terrestrially derived FDOM are known to be stable higher molecular weight aromatic compounds, generally considered non-labile (Cooper et al., 2016). However, recent work concerning the marine environment has suggested that humic-like FDOM could be a consequence of bacterial metabolism (Guillemette and del Giorgio, 2012; Kramer and Herndl, 2004; Romera-Castillo et al., 2011; Shimotori et al., 2012). Recent findings by Kallenbach et al. (2016) have shown the production of extracellular humic material by bacteria within soil organic matter. There is no direct evidence that the production of humic-like FDOM in freshwaters is the result of bacterial processing. However, Elliott et al. (2006) attributed the presence of this FOM in laboratory samples to stress as opposed to a function that may inherently occur within aquatic systems. What is clear from the literature is that a more detailed understanding of microbial/OM interactions in freshwater systems is needed.

Autochthonous and allochthonous FDOM can be associated with protein-like fluorescence ($\lambda_{ex}/\lambda_{em}$ 230-280/330-360 nm) specifically referred to as Peak T, $\lambda_{ex}/\lambda_{em}$275/340 nm, (tryptophan-like) and Peak A_T, $\lambda_{ex}/\lambda_{em}$ 230/305 nm, (tyrosine-like) (Coble et al., 2014). This

protein-like FDOM is attributed and assumed to be of microbial origin (Cammack et al., 2004; Coble et al., 2014; Hambly et al., 2015; Smith et al., 2004). Recent literature suggests that Peak T fluorescence may act as a surrogate for microbial and bacterial activity (Baker et al., 2015; Cumberland et al., 2012), as first highlighted by Hudson et al. (2008). Recent surface freshwater research has also attempted to use Peak T fluorescence to determine enumeration of specific species. For example, Baker et al. (2015) observed a log correlation R = 0.74 across a 7-log range in *Escherichia coli* enumeration for sewage impacted rivers. Using Peak T fluorescence to infer microbial enumeration, and activity, has been further suggested for groundwater systems, where there is little background fluorescence interference (Sorensen et al., 2016, 2015). Sorensen et al. (2015) investigated low levels of microbial contamination in drinking water supplies, reporting linear correlations, R^2 = 0.57 from < 2 to 700 cfu 100 ml^{-1}. Although relationships have been demonstrated for protein-like fluorescence and the presence of bacteria in freshwater systems, the research reported thus far does not take into account the implication and impact of microbial activity at an individual species level.

The study aim was to further our understanding of the role aquatic microbes play in the production of both protein-like and humic-like FOM in freshwaters. For this, we focus on the development of FOM in a model system using a simplified microbial community, thus removing the background complexities observed in environmental samples. Using this approach, we also determine the intracellular and extracellular fluorescence signatures of common freshwater bacterial species.

2 Methods

2.1 Bacterial species

Three bacterial species were cultured for analysis; *Escherichia coli* (ATCC 10536) was used as its presence in freshwaters can indicate sewage contamination (Sigee, 2004); *Bacillus subtilis* (ATCC 6633) was used as it is a ubiquitous soil bacterium (Graumann, 2007) that may be transferred into freshwater systems; and *Pseudomonas aeruginosa* (NCIMB 8295) as it is ubiquitous in freshwater systems (Elliott et al., 2006; Sigee, 2004).

2.2 Media

A non-fluorescent minimal media was developed to promote growth within our model system whilst excluding the presence of proteinaceous material. The basal medium consisted of a final concentration of 0.2% v/v glucose solution, as the sole carbon source, and a solution containing a source of phosphate, nitrogen, sodium and magnesium. The basal medium was adopted from the ATCC® medium 778 Davis and Mingioli minimal medium (Davis and Mingioli, 1950), but without the addition of amino acids and agar. All elements of the basal medium were filter sterilised using a Minisart® 0.2 µm cellulose filter (Sartorius Stedim Biotech, Germany). $CaCl_2$ (final concentration 0.035% v/v) and a trace element solution (final concentration 0.1% v/v), obtained from Kragelund and Nybroe (1994), were added to the sterile basal medium prior to inoculation. These chemicals were sterilised by autoclaving at 121°C for 15 minutes.

2.3 Fluorescence measurements

Fluorescence excitation-emission matrices (EEMs) were collected using an Aqualog ® (Horiba Ltd., Japan). Samples were not filtered prior to fluorescence spectroscopic analysis

(except for bacterial supernatant samples, section 2.6). The scan parameters employed were; excitation wavelengths from 200 to 500 nm via 1 nm steps, and emission wavelengths of 247.88 to 829.85 nm in 1.16 nm steps using an integration time of 500 milliseconds. A micro quartz cuvette (1400 µL) with a 10 mm path-length was used throughout. Spectra were blank subtracted, corrected for inner filter effects (for both excitation and emission wavelengths) and first and second order Rayleigh Scattering masked (±10 nm at $\lambda_{ex}=\lambda_{em}$ and $2\lambda_{ex}=\lambda_{em}$) (Coble et al., 2014; McKnight et al., 2001). Fluorescence data is reported in quinine sulphate units (QSU), determined from normalising data to the fluorescence from 1 µg L^{-1} quinine sulphate at λ_{ex} = 347.5 nm and λ_{em} = 450 nm (Kramer and Herndl, 2004; Mostofa et al., 2013; Shimotori et al., 2012, 2009). Instrument validation was undertaken daily with a quinine sulphate standard (Starna Cells, USA), with CV being < 3% (n = 5) in all events.

2.4 Fluorescence data analysis

A custom script, written in Python™ (Python Software Foundation), was used to convert the data into QSU and create the EEM maps. The script crops the data window to λ_{ex} 240-490 nm, λ_{em} 250-550 nm to allow for the analysis of the UV spectra, the area of interest within FDOM work. Data λ_{ex} <240 nm was discounted due to the data quality produced by the Aqualog® caused by the signal to noise ratio. The custom script was then used to undertake peak picking for specific fluorescence peaks. Some of the peak picked data was normalised to the maxima to provide a clear visual representation of the fluorescence development over time. The EEM data was also investigated by employing parallel factor (PARAFAC) analysis (Stedmon and Bro, 2008) in Solo (Eigenvector Research Inc., WA, USA) software, in conjunction with the MATLAB® PLS-Toolbox (Mathworks, USA).

2.5 Bacterial growth curves

Growth curves (n = 9 i.e. nine independent replicates) of each bacterial species were undertaken by inoculating 150 mL of the sterile medium (section 2.2) from a fresh overnight plate culture (< 24 hours) and incubating the samples at 37°C, shaking at 150 rpm. Aliquots were collected every 30 minutes for fluorescence measurements (section 2.3) and optical density (OD) measurements at 600 nm (WPA Spectrawave S1200, Biochrom, UK); OD, attenuation determined by absorbance and scattering, is routinely used to represent the relative increase in cell numbers within a sample when monitoring bacterial growth (Hall et al., 2014). OD data was also normalised to the maxima.

2.6 Bacterial culture analysis

Media was inoculated, from a fresh overnight plate culture (< 24 hours), with each of the bacterial species and incubated overnight at 37°C, shaking at 150 rpm throughout. Overnight cultures were centrifuged at 5000 x g for 5 minutes (Allegra X-30R, Beckman Coulter™, USA) to form a bacterial pellet. The supernatant was pipetted off and filtered using a Minisart® 0.2 µm cellulose filter (Sartorius Stedim Biotech, Germany) to guarantee all cells were removed. The pellet was resuspended and washed 3 times in 5 mL of ¼ strength Ringer solution (Oxoid Ltd., UK) to ensure that any supernatant or media was no longer present. To physically lyse the cells, a 1 mL aliquot of the resuspended cells was sonicated (Ultrasonic Processor XL 2020, Misonix Inc., US) in three 10 second pulses at a fixed frequency of 20 KHz, not exceeding 40% amplitude, and kept over ice throughout (Doron, 2009). Physical lysis was undertaken to ensure no extra chemicals were added to the cells that may alter the fluorescence properties of the sample (nine independent replicates). An endospore suspension for *B. subtilis* was prepared as described by Lawrence and Palombo (2009). To check for the presence of endospores and the removal of

169 vegetative cells, an endospore stain was conducted using the Schaeffer-Fulton method
170 (Schaeffer and Fulton, 1933).

3 Results and Discussion

Filtering of samples was not performed prior to spectroscopic analysis to maintain sample integrity (Baker et al., 2007), since the focus of this study is on *in situ* bacterial production of FOM in a model system. Each individual bacterial species exhibited unique fluorescing signatures. Some FOM, specifically Peak T, was dominant in all samples exhibiting high fluorescence intensities. This limited the application of PARAFAC analysis, whereby no robust model, CORCONDIA >90% (Bro and Kiers, 2003), that adequately explained the dataset could be identified. Subsequently, peak picking (Asmala et al., 2016), an established method for spectral analysis, was applied to peaks identified within the EEMs.

3.1 Bacterial growth curves

3.1.1 Escherichia coli

The *E. coli* growth curve is shown in Figure 1, whereby Peak T is the dominant fluorescence peak and is present at time zero, upon initial addition of the *E. coli* cells (Dartnell et al., 2013; Sohn et al., 2009). During the growth curve, the intensity of Peak T increases in line with the optical density (OD) of the sample (Figure 1). During the exponential stage (growth phase after acclimatisation; Hogg, 2005) there is a log increase in the intensity of Peak T fluorescence. This, alongside the increase in OD, leads to a significant strong correlation between Peak T and OD, $R^2 = 0.9821$ ($p < 0.001$). This suggests that Peak T fluorescence intensity can be attributed to an increase in *E. coli* population size, in accordance with previous studies (Baker et al., 2015; Cumberland et al., 2012; Dartnell et al., 2013; Deepa and Ganesh, 2017; Sohn et al., 2009). However, as tryptophan is an essential amino acid, necessary for protein formation during growth and other metabolic pathways, it will be produced as a result of cell multiplication and metabolic processing (Coble et al., 2014; Hogg, 2005). As such, Peak T fluorescence can also be attributed to *E. coli* cell activity.

196 Figure 1 shows that Peak C also develops during the exponential phase of the growth curve,
197 exhibiting a lag in relation to the OD. The intensity of Peak C continues to increase even
198 during stationary phase, in which cell deaths are equal to newly formed cells (Elliott et al.,
199 2006; Hogg, 2005). Nevertheless a positive correlation between OD and Peak C
200 fluorescence intensity is identified, $R^2 = 0.8624$ ($p < 0.001$), supporting the association of
201 Peak C with bacterial numbers. However, the observed lag in conjunction with the continued
202 increase in fluorescence intensity during the stationary phase strongly supports the idea that
203 metabolic activity, and not bacterial numbers *per se*, may be the main driver for the creation
204 and production of Peak C fluorophores. Notably, the observed maximum fluorescence
205 intensity of Peak C is a factor of 10 lower than Peak T (Figure 1a). It can, therefore, be
206 suggested that Peak C may be derived as a metabolic by-product or a secondary metabolite
207 produced mainly during the stationary phase (Figure 1b). Peak X (Table 1) is only present
208 within the stationary phase, albeit at comparatively low fluorescence intensities (~ 30 QSU).
209 The microbial production of Peaks C and X demonstrates the ability of *E. coli* to rapidly
210 produce (within eight hours), *in situ*, FOM associated with allochthonous high molecular
211 weight FOM.

212

213 *3.1.2 Bacillus subtilis*

214 Figure 2 highlights Peak T as the dominant fluorescence peak within the *B. subtilis* growth
215 curve. Peak T intensity increases by an order of magnitude throughout the growth curve, in
216 line with the increased OD (Figure 2), demonstrating a strong significant correlation, $R^2 =$
217 0.9879 ($p < 0.005$). However, as Peak T fluorescence intensity increases during what
218 appears to be early stationary phase (Figure 2), it could be suggested that these
219 fluorophores are produced by metabolically active cells. This emphasises the use of Peak T
220 as an indicator of microbial activity rather than being attributed to cell enumeration, despite
221 the significant correlation identified. The production of Peak T within the stationary phase

222 (Figure 2) could also be related to *B. subtilis* sporulation, demonstrated by the high intensity
223 Peak T fluorescence obtained bacterial endospores analysed alone (Figure 3). This
224 suggests that some of the fluorophores attributable to Peak T fluorescence are related to
225 structural proteins since endospores are not metabolically active, although this is species
226 specific.

227 Within the *B. subtilis* growth curve, Peak C demonstrates a sudden rise, at 360 minutes,
228 prior to OD and Peak T development (Figure 2), with a strong positive correlation between
229 Peak C fluorescence intensity and the OD being identified, $R^2 = 0.9465$ ($p < 0.005$). This
230 further challenges our current understanding of Peak C being attributed to terrestrial
231 allochthonous material (Coble et al., 2014). Smith et al. (2004) suggested that the Peak C
232 fluorescence, identified in the presence of *Bacillus sp.,* may be related to the fluorescence of
233 endospores. However, Figure 3 demonstrates the endospore suspension obtained from *B.*
234 *subtilis* within our study as having high Peak T, and low Peak C, fluorescence intensity.

235 Florescence Peaks M and A_M are produced and observed at very low intensities within the
236 early stationary phase of the growth curve. A possible explanation of this observation is the
237 result of the biodegradation of OM responsible for Peak C fluorescence, a process that has
238 been noted in the literature (Coble et al., 2014). Alternatively, this could indicate that Peaks
239 M and A_M can be produced directly, *in situ*, by bacteria, as has been suggested to occur
240 within marine environments (Coble, 1996; Shimotori et al., 2009).

241

242 *3.1.3 Pseudomonas aeruginosa*

243 Peak T is ubiquitous within the *P. aeruginosa* growth curve (Figure 4), increasing by an order
244 of magnitude within the exponential phase. A relatively weaker correlation, $R^2 = 0.7601$ ($p <$
245 0.005), is identified between Peak T and the OD, likely to be caused by the upregulation of
246 Peak T independent of cell number which can be seen at 330 minutes, in the late

247 exponential, early stationary phase (Figure 4). Prior to this, the Peak T fluorescence
248 development tracks the OD (R^2 = 0.9674, $p < 0.05$). One possible explanation for this
249 sudden increase in Peak T fluorescence intensity is the production of exotoxin A; exotoxin A
250 is an iron-scavenging enzyme that is produced by *P. aeruginosa* upon entry into stationary
251 phase (Lory, 1986; Somerville et al., 1999). Previous studies have shown how Exotoxin A
252 can be used to determine protein activity, by assessing tryptophan (Peak T) fluorescence
253 quenching upon binding of NAD+ to the enzyme active site (Beattie and Merrill, 1999, 1996;
254 Beattie et al., 1996). Therefore, the observed subsequent sudden decline in Peak T
255 fluorescence intensity at 450 minutes may be as a result of this quenching phenomena
256 (Figure 4).

257 *P. aeruginosa* has the most complex EEM spectra of the species analysed within this study
258 (Dartnell et al., 2013; Elliott et al., 2006; Smith et al., 2004), with Peaks T, C and A_C all
259 immediately identified upon inoculation and during the lag phase (a period of acclimatisation;
260 Hogg, 2005). The occurrence of Peaks C and A_C at inoculation suggests it is likely that this
261 FDOM is intracellular and produced within the cells during the initial overnight incubation;
262 likely to be structural or functional proteins produced via microbial metabolic pathways, or
263 potentially intracellular metabolic by-products. These peaks increase log-fold throughout the
264 growth curve, with both Peaks C and A_C being correlated with, despite a lag in relation to, the
265 OD; R^2 = 0.7024 ($p < 0.005$) and R^2 = 0.7146 ($p < 0.005$) respectively. The data indicates
266 upregulation of these peaks during late exponential phase and stationary phase, suggesting
267 that these peaks are a result of metabolic activity.

268 Peak C+ develops rapidly and to a high intensity during the stationary phase of *P.*
269 *aeruginosa* growth (Figure 4) and this fluorescent peak is associated with the siderophore
270 pyoverdine (Dartnell et al., 2013; Wasserman, 1965). Pyoverdine is an extracellular iron-
271 scavenging metabolite produced by *P. aeruginosa* and is associated with microbial virulence
272 (da Silva and de Almeida, 2006). The fluorescence intensity of this high molecular weight
273 OM within the *P. aeruginosa* growth curve, suggests that this Peak C+ fluorescence could

be derived from the building and exporting of pyoverdine. Peak C+ has been seen in freshwater environments and is currently attributed to terrestrial allochthonous OM. However, our work proves that microbial compounds produced *in situ* (akin to autochthonous material) may contribute to this Peak C+ fluorescence. As such, Peak C+ may act as a biomarker for an active *P. aeruginosa* community, although further investigation within natural environmental systems is required.

3.2 Overnight culturing of bacterial species

From the microbial growth curve data it has been shown that all the fluorescence peaks identified (Table 1) are microbially produced *in situ*, with variations in peak occurrence between bacterial species. To further investigate the microbial source and origin of the OM, overnight cultures of each species were analysed to determine the presence of FDOM in the supernatant, OM within resuspended cells and lysed cells (see section 2.6). This provides a preliminary understanding of where the observed fluorescence is located post FOM production.

Peak T fluorescence is the only ubiquitous fluorescence peak common to all bacterial species cultured overnight (Table 2). This shows that the intensity of Peak T alone cannot be used to determine bacterial enumeration, especially in systems with complex microbial communities, but supports its use as a measure of microbial activity. The highest intensity for Peak T fluorescence is seen within the resuspended and lysed cells, suggesting that the majority of this material is intracellular, either as structural or functional biological molecules. This explains the presence of Peak T upon inoculation and the increase in intensity with cell multiplication (section 3.1). However, the presence of Peak T in the supernatant also indicates that some of this fluorescence signal is derived from extracellular FDOM, although the amount is species specific, varying from 5-25%. This material is possibly associated with

299 metabolic by-products or extracellular proteins (many of which may be functional) that have
300 been exported from the cells.

301 Peak C fluorescence was observed in both the supernatant and cell lysis fractions for *E. coli*
302 and *B. subtilis* (shown in Table 2). Within the supernatant fraction, this can be attributed to
303 either (1) material exported out of the cell (either functional proteins or metabolic by-
304 products) or (2) cellular debris as a result of cell lysis during growth (prior to sampling).
305 However, Peak C fluorescence may also be derived from compounds that fluoresce when
306 not bound within a cell where the fluorescence signal is quenched or inhibited. Peak C is
307 present in all elements of the *P. aeruginosa* culture, indicating that for this species this FOM
308 is likely to be a functional protein that can be exported to become extracellular DOM.
309 Collectively, this data indicates that the fluorophores that give rise to Peak C fluorescence
310 may be derived from either cell lysis (Elliott et al., 2006) or attributed to microbial metabolic
311 by-products or extracellular proteins (Guillemette and del Giorgio, 2012; Shimotori et al.,
312 2009).

313 Peak A_C is also seen in all fractions of the *P. aeruginosa* culture and in the *E. coli*
314 supernatant. This suggests that this FOM may be a function of a particular biological
315 molecule(s) common to both *P. aeruginosa* and *E. coli*. Peak C+ was also observed in the *E.*
316 *coli* supernatant, but at far lower levels compared to *P. aeruginosa*. The high fluorescence
317 intensity of Peak C+ in all elements of the *P. aeruginosa* culture, and the association of this
318 peak with pyoverdine (section 3.1), demonstrates the possible intracellular production and
319 extracellular output of this FOM. Peak M is also observed within all fractions of the *P.*
320 *aeruginosa* culture, but is only present in the *B. subtilis* supernatant. This suggests it may
321 have a similar species specific function like Peak A_C, or be derived via the biodegradation of
322 Peak C (Coble, 1996; Coble et al., 2014). As the fluorophores attributed to these peaks (T,
323 C, A_C, C+ and M) can be exported from cells and are identified in cells, lysed cell material
324 and supernatant, they are unlikely to represent cellular structural material. Whilst Peak M is
325 identified in relation to both *B. subtilis* and *P. aeruginosa*, Peak A_M is only observed in the

supernatant of *P. aeruginosa*, although these peaks have been seen to occur simultaneously in the environment (Coble et al., 2014). Therefore, Peak A_M could be attributed to either species specific proteins or bacterial metabolic by-products. From this, Peaks M and A_M must be considered separately as they are likely derived from different fluorophores.

Although noted in previous life science research (Smith et al., 2004), Peak X (Table 1) has not yet been reported or characterised in aquatic FDOM. However, it is identified at low fluorescence intensities in the supernatant for all species analysed within this study (Table 2). Based on our current understanding of fluorophore structures (Lakowicz, 2006), it is likely that this peak is derived from high molecular weight compounds (characterised as humic and fulvic acids), that would usually be attributed to terrestrial allochthonous material in the environment. Nevertheless, as it is only seen in the supernatant it is likely to be secreted from the cells and not related to cellular structure.

3.3 Future work

The protein-like fluorescence region has been the focus for research investigating microbially-derived, autochthonous dissolved organic matter. The data from this study furthers our current understanding of bacteria-OM interactions and highlights the importance of metabolic activity and bacterial population growth for driving the dynamics of microbially produced FOM and FDOM, albeit within a model system. Furthermore the bacterially derived FOM, exhibits the same fluorescent features as DOM observed in natural systems which has previously been attributed as being allochthonous in origin. This work raises questions regarding the extent to which bacterially produced FOM occurs in freshwater systems and the role that any production plays in the biogeochemical cycling throughout the hydrological continuum. Finally, further work should also explore the metabolic pathways responsible for

351 the microbial production and transformation of FOM and FDOM, including optical regions
352 that are limited by the instrumentation used in this study (e.g. λ_{ex} 200-240 nm).

4 Conclusions

- Peak T fluorescence correlates strongly with an increasing bacterial population, but is dependent on microbial metabolic activity. As such, we suggest Peak T as a proxy for microbial activity rather than enumeration.

- This work provides direct evidence that Peak T fluorescence is ubiquitous within the bacterial cells analysed within this study. It is mainly identified as intracellular material but also exists as extracellular FDOM.

- Peak C is produced *in situ* during the exponential stage of bacterial growth curves, likely to be produced via microbial metabolic pathways during microbial growth, or derived from metabolic by-products.

- FOM peaks can be partially attributed to microbial metabolic processing, through the production of biological molecules, some of which is exported from the cell. These FOM peaks include regions that are currently associated with allochthonous high molecular weight compounds, categorised as humic and fulvic acids.

- FOM production varies between bacterial species, with this work providing definitive evidence that freshwater FOM can be produced by microbes *in situ.* It can therefore be of autochthonous origin, altering and enhancing our understanding regarding the complexity of environmental OM origin.

- Extracellular organic matter contributes to FDOM and, as such, is available as an organic matter source for microorganisms, playing an essential role in nutrient exchange and global carbon cycling.

374 Acknowledgements

375 This work was funded by the Natural Environmental Research Council (NERC) and Chelsea
376 Technologies Group Ltd as a CASE Award (NE/K007572/1).

377 References

378 Asmala, E., Kaartokallio, H., Carstensen, J., Thomas, D.N., 2016. Variation in Riverine
379 Inputs Affect Dissolved Organic Matter Characteristics throughout the Estuarine
380 Gradient. Front. Mar. Sci. 2, 1–15. doi:10.3389/fmars.2015.00125

381 Baker, A., 2005. Thermal fluorescence quenching properties of dissolved organic matter.
382 Water Res. 39, 4405–4412. doi:10.1016/j.watres.2005.08.023

383 Baker, A., Cumberland, S.A., Bradley, C., Buckley, C., Bridgeman, J., 2015. To what extent
384 can portable fluorescence spectroscopy be used in the real-time assessment of
385 microbial water quality? Sci. Total Environ. 532, 14–19.
386 doi:10.1016/j.scitotenv.2015.05.114

387 Baker, A., Elliott, S., Lead, J.R., 2007. Effects of filtration and pH perturbation on freshwater
388 organic matter fluorescence. Chemosphere 67, 2035–2043.
389 doi:10.1016/j.chemosphere.2006.11.024

390 Beattie, B.K., Merrill, A.R., 1999. A Fluorescence Investigation of the Active Site of
391 *Pseudomonas aeruginosa* Exotoxin A. J. Biol. Chem. 274, 15646–15654.
392 doi:10.1074/jbc.274.22.15646

393 Beattie, B.K., Merrill, A.R., 1996. *In vitro* Enzyme Activation and Folded Stability of
394 *Pseudomonas aeruginosa* Exotoxin A and Its C-Terminal Peptide. Biochemistry 35,
395 9042–9051. doi:10.1021/bi960396k

396 Beattie, B.K., Prentice, G.A., Merrill, A.R., 1996. Investigation into the Catalytic role for the
397 Tryptophan Residues within Domain III of *Pseudomonas aeruginosa* Exotoxin A.
398 Biochemistry 35, 15134–15142. doi:10.1021/bi961985t

399 Bieroza, M.Z., Heathwaite, A.L., 2016. Unravelling organic matter and nutrient
400 biogeochemistry in groundwater-fed rivers under baseflow conditions: Uncertainty in *in*

401 *situ* high-frequency analysis. Sci. Total Environ. doi:10.1016/j.scitotenv.2016.02.046

402 Bridgeman, J., Baker, A., Brown, D., Boxall, J.B., 2015. Portable LED fluorescence
403 instrumentation for the rapid assessment of potable water quality. Sci. Total Environ.
404 524-525, 338–346. doi:10.1016/j.scitotenv.2015.04.050

405 Bro, R., Kiers, H.A.L., 2003. A new efficient method for determining the number of
406 components in PARAFAC models. J. Chemom. 17, 274–286. doi:10.1002/cem.801

407 Cammack, W.K.L., Kalff, J., Prairie, Y.T., Smith, E.M., 2004. Fluorescent dissolved organic
408 matter in lakes: Relationships with heterotrophic metabolism. Limnol. Oceanogr. 49,
409 2034–2045. doi:10.4319/lo.2004.49.6.2034

410 Coble, P.G., 1996. Characterization of marine and terrestrial DOM in seawater using
411 excitation-emission matrix spectroscopy. Mar. Chem. 51, 325–346. doi:10.1016/0304-
412 4203(95)00062-3

413 Coble, P.G., Lead, J., Baker, A., Reynolds, D.M., Spencer, R.G.M., 2014. Aquatic Organic
414 Matter Fluorescence. Cambridge University Press.

415 Cooper, K.J., Whitaker, F.F., Anesio, A.M., Naish, M., Reynolds, D.M., Evans, E.L., 2016.
416 Dissolved organic carbon transformations and microbial community response to
417 variations in recharge waters in a shallow carbonate aquifer. Biogeochemistry 129,
418 215–234. doi:10.1007/s10533-016-0226-4

419 Cumberland, S., Bridgeman, J., Baker, A., Sterling, M., Ward, D., 2012. Fluorescence
420 spectroscopy as a tool for determining microbial quality in potable water applications.
421 Environ. Technol. 33, 687–693. doi:10.1080/09593330.2011.588401

422 da Silva, G.A., de Almeida, E.A., 2006. Production of Yellow-Green Fluorescent Pigment by
423 *Pseudomonas fluorescens*. Brazilian Arch. Biol. Technol. 49, 411–419.
424 doi:10.1590/S1516-89132006000400009

425 Dartnell, L.R., Roberts, T.A., Moore, G., Ward, J.M., Muller, J.P., 2013. Fluorescence
426 Characterization of Clinically-Important Bacteria. PLoS One 8, 1–13.
427 doi:10.1371/journal.pone.0075270

428 Davis, B.D., Mingioli, E.S., 1950. Mutants of Escherichia coli requiring methionine or vitamin
429 B12. J. Bacteriol. 60, 17–28.

430 Deepa, N., Ganesh, A.B., 2017. Minimally invasive fluorescence sensing system for real-
431 time monitoring of bacterial cell cultivation. Instrum. Sci. Technol. 45, 85–100.
432 doi:10.1080/10739149.2016.1198372

433 Doron, N., 2009. Sonication of bacterial samples [WWW Document]. URL
434 http://wolfson.huji.ac.il/expression/procedures/cell_lysis/Sonication_of_bacterial_sampl
435 es.html (accessed 8.10.16).

436 Elliott, S., Lead, J.R., Baker, A., 2006. Characterisation of the fluorescence from freshwater,
437 planktonic bacteria. Water Res. 40, 2075–2083. doi:10.1016/j.watres.2006.03.017

438 Graumann, P. (Ed.), 2007. *Bacillus*: Cellular and Molecular Biology. Caister Academic Press.

439 Guillemette, F., del Giorgio, P.A., 2012. Simultaneous consumption and production of
440 fluorescent dissolved organic matter by lake bacterioplankton. Environ. Microbiol. 14,
441 1432–1443. doi:10.1111/j.1462-2920.2012.02728.x

442 Hall, B.G., Acar, H., Nandipati, A., Barlow, M., 2014. Growth Rates Made Easy. Mol. Biol.
443 Evol. 31, 232–238. doi:10.1093/molbev/mst187

444 Hambly, A.C., Arvin, E., Pedersen, L.F., Pedersen, P.B., Seredyńska-Sobecka, B., Stedmon,
445 C.A., 2015. Characterising organic matter in recirculating aquaculture systems with
446 fluorescence EEM spectroscopy. Water Res. 83, 112–120.
447 doi:10.1016/j.watres.2015.06.037

448 Hogg, S., 2005. Essential Microbiology. Wiley.

449 Hudson, N., Baker, A., Reynolds, D.M., 2007. Fluorescence Analysis of Dissolved Organic
450 Matter in Natural, Waste and Polluted Water - A Review. River Res. Appl. 23, 631–649.
451 doi:10.1002/rra.1005

452 Hudson, N., Baker, A., Ward, D., Reynolds, D.M., Brunsdon, C., Carliell-Marquet, C.,
453 Browning, S., 2008. Can fluorescence spectrometry be used as a surrogate for the
454 Biochemical Oxygen Demand (BOD) test in water quality assessment? An example
455 from South West England. Sci. Total Environ. 391, 149–158.
456 doi:10.1016/j.scitotenv.2007.10.054

457 Kallenbach, C.M., Frey, S.D., Grandy, A.S., 2016. Direct evidence for microbial-derived soil
458 organic matter formation and its ecophysiological controls. Nat. Commun. 7, 1–10.
459 doi:10.1038/ncomms13630

460 Kragelund, L., Nybroe, O., 1994. Culturability and Expression of Outer Membrane Proteins
461 during Carbon, Nitrogen, or Phosphorus Starvation of *Pseudomonas fluorescens* DF57
462 and *Pseudomonas putida* DF14. Appl. Environ. Microbiol. 60, 2944–2948.

463 Kramer, G.D., Herndl, G.J., 2004. Photo- and bioreactivity of chromophoric dissolved organic
464 matter produced by marine bacterioplankton. Aquat. Microb. Ecol. 36, 239–246.

465 Lakowicz, J.R., 2006. Principles of Fluorescence Spectroscopy, 3rd ed. Springer.
466 doi:10.1007/978-0-387-46312-4

467 Lawrence, H.A., Palombo, E.A., 2009. Activity of Essential Oils Against *Bacillus subtilis*
468 spores. J. Microbiol. Biotechnol. 19, 1590–1595. doi:10.4014/jmb.0904.04016

469 Lory, S., 1986. Effect of Iron on Accumulation of Exotoxin A-Specific mRNA in
470 *Pseudomonas aeruginosa*. J. Bacteriol. 168, 1451–1456.

McKnight, D.M., E. W. Boyer, P. K. Westerhoff, P. T. Doran, T. Kulbe, Anderson, D.T., 2001. Spectroflourometric characterization of dissolved organic matter for indication of precursor organic material and aromaticity. Limnol. Oceanogr. 46, 38–48.

Mostofa, K.M.G., Yoshioka, T., Mottaleb, A., Vione, D., 2013. Photobiogeochemistry of Organic Matter: Principles and Practices in Water Environments. Springer.

Romera-Castillo, C., Sarmento, H., Alvarez-Salgado, X.A., Gasol, J.M., Marrasé, C., 2011. Net Production and Consumption of Fluorescent Colored Dissolved Organic Matter by Natural Bacterial Assemblages Growing on Marine Phytoplankton Exudates. Appl. Environ. Microbiol. 77, 7490–7498. doi:10.1128/AEM.00200-11

Schaeffer, A.B., Fulton, M.D., 1933. A Simplified Method of Staining Endospores. Science (80-.). 77, 194. doi:10.1126/science.77.1990.194

Shimotori, K., Omori, Y., Hama, T., 2009. Bacterial production of marine humic-like fluorescent dissolved organic matter and its biogeochemical importance. Aquat. Microb. Ecol. 58, 55–66. doi:10.3354/ame01350

Shimotori, K., Watanabe, K., Hama, T., 2012. Fluorescence characteristics of humic-like fluorescent dissolved organic matter produced by various taxa of marine bacteria. Aquat. Microb. Ecol. 65, 249–260. doi:10.3354/ame01552

Sigee, D.C., 2004. Freshwater Microbiology. Wiley.

Smith, C.B., Anderson, J.E., Webb, S.R., 2004. Detection of *Bacillus* endospores using total luminescence spectroscopy. Spectrochim. Acta - Part A Mol. Biomol. Spectrosc. 60, 2517–2521. doi:10.1016/j.saa.2003.12.030

Sohn, M., Himmelsbach, D.S., Barton, F.E.I., Fedorka-Cray, P.J., 2009. Fluorescence Spectroscopy for Rapid Detection and Classification of Bacterial Pathogens. Appl. Spectrosc. 63, 1251–1255.

Somerville, G., Mikoryak, C.A., Reitzer, L., Mikoryak, C.A.N.N., 1999. Physiological Characterization of *Pseudomonas aeruginosa* during Exotoxin A Synthesis: Glutamate, Iron Limitation, and Aconitase Activity. J. Bacteriol. 181, 1072–1078.

Sorensen, J.P.R., Lapworth, D.J., Marchant, B.P., Nkhuwa, D.C.W., Pedley, S., Stuart, M.E., Bell, R.A., Chirwa, M., Kabika, J., Liemisa, M., Chibesa, M., 2015. *In situ* tryptophan-like fluorescence: A real-time indicator of faecal contamination in drinking water supplies. Water Res. 81, 38–46. doi:10.1016/j.watres.2015.05.035

Sorensen, J.P.R., Sadhu, A., Sampath, G., Sugden, S., Dutta Gupta, S., Lapworth, D.J., Marchant, B.P., Pedley, S., 2016. Are sanitation interventions a threat to drinking water supplies in rural India? An application of tryptophan-like fluorescence. Water Res. 88, 923–932. doi:10.1016/j.watres.2015.11.006

Stedmon, C.A., Bro, R., 2008. Characterizing dissolved organic matter fluorescence with paral lel factor analysis : a tutorial. Limnol. Oceanogr. Methods 6, 572–579. doi:10.4319/lom.2008.6.572

Wasserman, A.E., 1965. Absorption and Fluorescence of Water-Soluble Pigments Produced by Four Species of *Pseudomonas*. Appl. Microbiol. 13, 175–180.

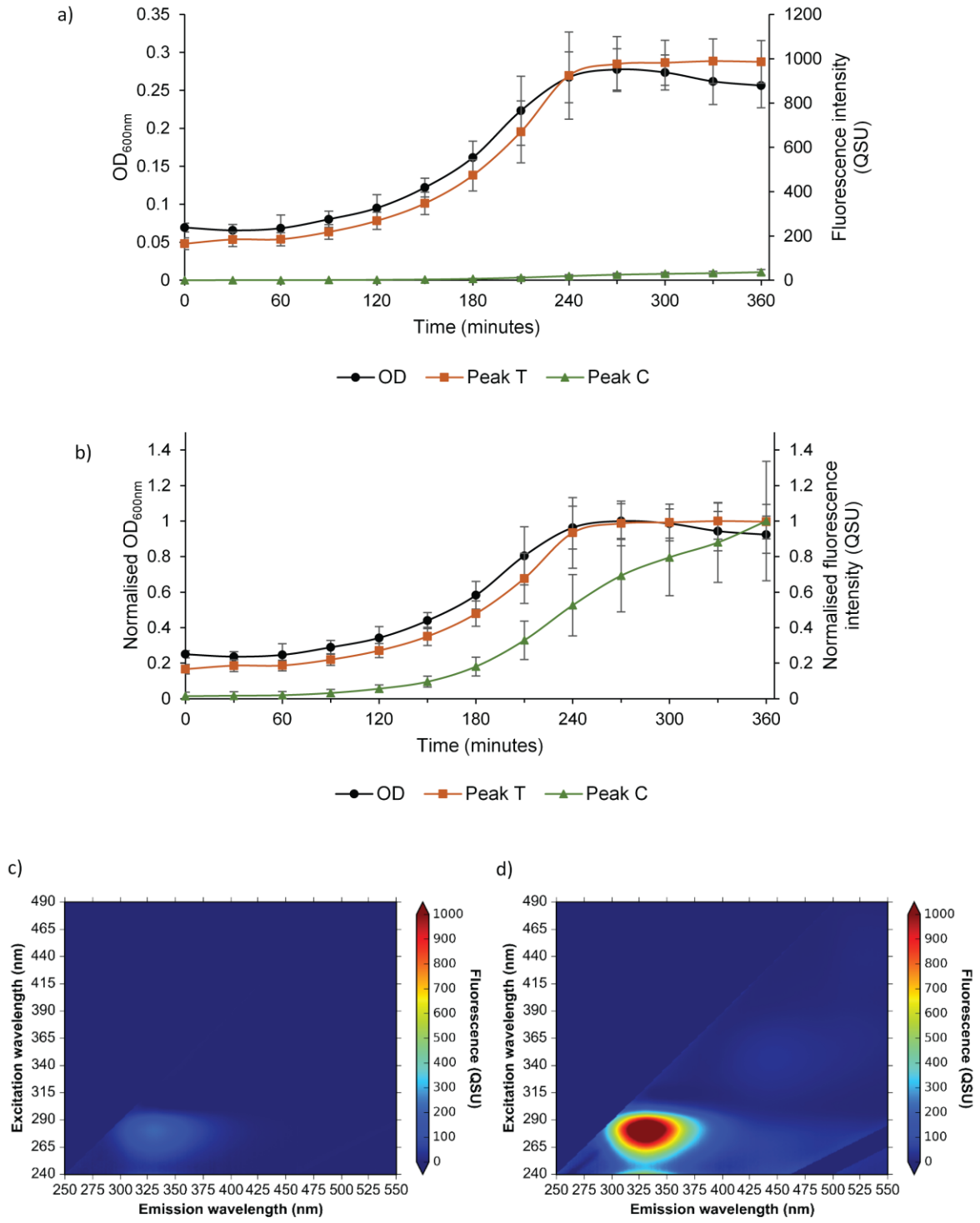

Figure 1: Fluorescence and optical density (OD_{600nm}) data for *Escherichia coli* growth curve, showing: a) optical density and fluorescence (QSU, 1 QSU = 1 μg^{-1} quinine sulphate) ± 1 standard deviation (n = 9); b) optical density and fluorescence data normalised to the maximum value ± 1 standard deviation (n = 9); c) excitation-emission matrix at time zero; and d) excitation-emission matrix at 360 minutes.

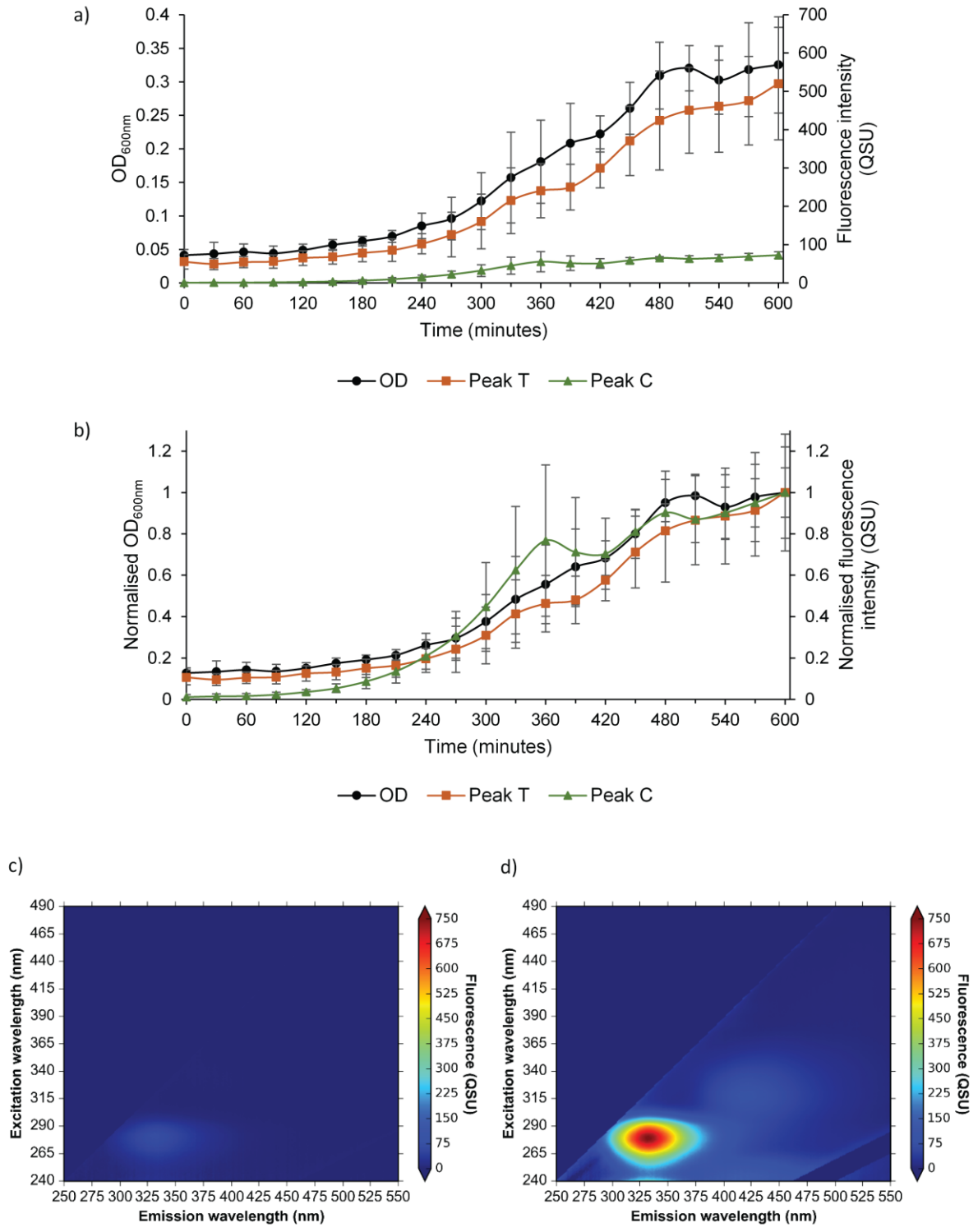

Figure 2: Fluorescence and optical density (OD_{600nm}) data for *Bacillus subtilis* growth curve, showing: a) optical density and fluorescence (QSU, 1 QSU = 1 μg^{-1} quinine sulphate) ± 1 standard deviation (n = 9); b) optical density and fluorescence data normalised to the maximum value ± 1 standard deviation (n = 9); c) excitation-emission matrix at time zero; and d) excitation-emission matrix at 360 minutes.

516

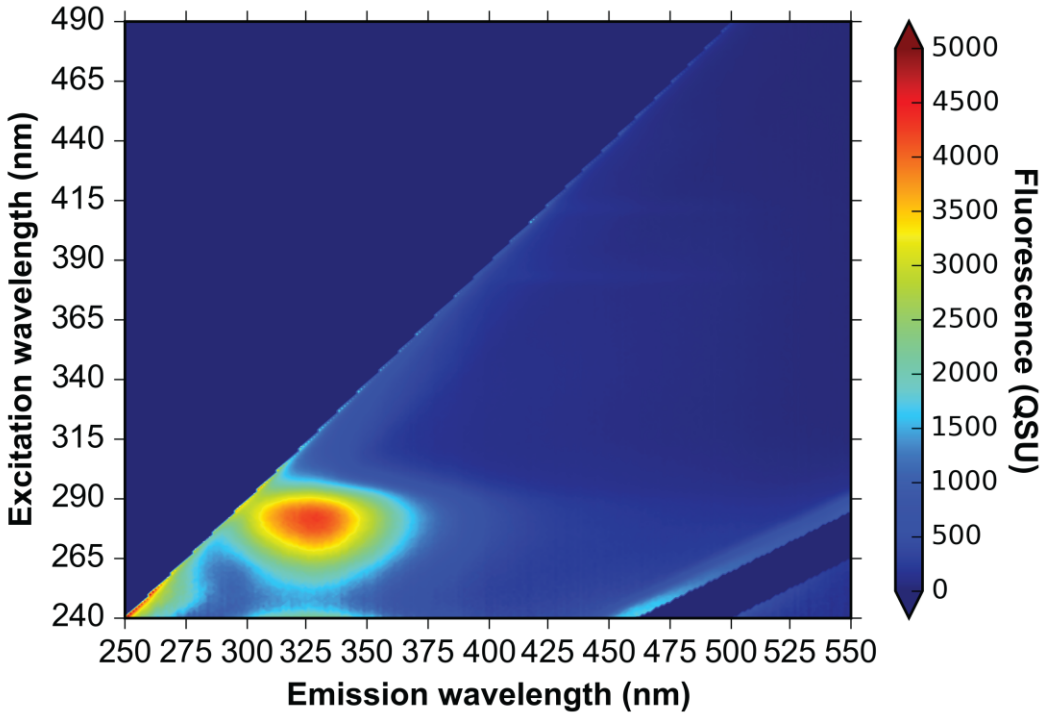

Figure 3: Fluorescence excitation-emission matrix of *Bacillus subtilis* endospores (QSU, 1 QSU = 1 μg^{-1} quinine sulphate).

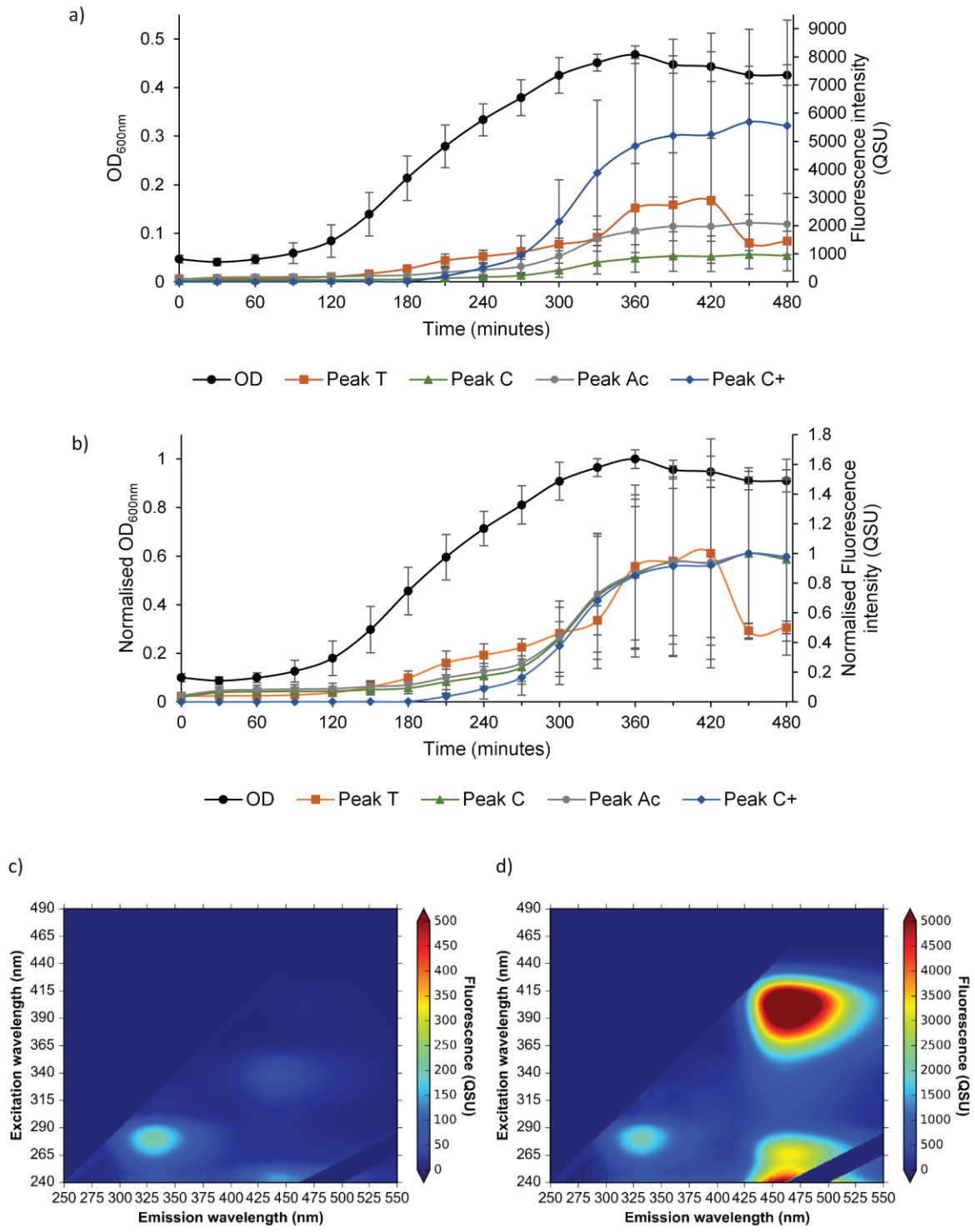

Figure 4: Fluorescence and optical density (OD_{600nm}) data for *Pseudomonas aeruginosa* growth curve, showing: a) optical density and fluorescence (QSU, 1 QSU = 1 μg^{-1} quinine sulphate) ± 1 standard deviation (n = 9); b) optical density and fluorescence data normalised to the maximum value ± 1 standard deviation (n = 9); c) excitation-emission matrix at time zero; and d) excitation-emission matrix at 360 minutes.